

RESEARCH

Open Access

In-vehicle channel sounding in the 5.8-GHz band

Pavel Kukolev¹, Aniruddha Chandra^{1*}, Tomáš Mikulášek¹, Aleš Prokeš¹, Thomas Zemen^{2,3}
and Christoph F Mecklenbräuer⁴

Abstract

The article reports vehicular channel measurements in the frequency band of 5.8 GHz for IEEE 802.11p standard. Experiments for both intra-vehicle and out-of-vehicle environments were carried out. It was observed that the large-scale variations (LSVs) of the power delay profiles (PDPs) can be best described through a two-term exponential decay model, in contrast to the linear models which are suitable for popular ultra-wideband (UWB) systems operating in the 3- to 11-GHz band. The small-scale variations (SSVs) are separated from the PDP by subtracting the LSV and characterized utilizing logistic, generalized extreme value (GEV), and normal distributions. Two sample Kolmogorov-Smirnov (K-S) tests validated that the logistic distribution is optimal for in-car, whereas the GEV distribution serves better for out-of-car measurements. For each measurement, the LSV trend was used to construct the respective channel impulse response (CIR), i.e., tap gains at different delays. Next, the CIR information is fed to an 802.11p simulation testbed to evaluate the bit error rate (BER) performance, following a Rician model. The BER results strongly vouch for the suitability of the protocol for in-car as well as out-of-car wireless applications in stationary environments.

Keywords: Intra-vehicle channel; IEEE 802.11p; Channel sounding; Ultra-wideband; Power delay profile; Bit error rate

1 Introduction

1.1 Motivation

Vehicle area networks (VANs) and vehicular *ad hoc* networks (VANETs) generally refer to networks between cars and infrastructure points located along the road side [1,2]. These networks are aimed to deliver information about the traffic, to ensure safety of the passengers, and to provide driver assistance and passenger entertainment [3]. The majority of future vehicular networks are envisaged to conform with the IEEE 802.11p standard [4] described in wireless access in vehicular environments (WAVE) [5] and governed by a non-profit organization, the car-2-car communication consortium (C2C-CC) [6]. IEEE 802.11p standardizes signal transmission for vehicle-to-vehicle (V2V) or vehicle-to-infrastructure (V2I) communications, operated at a frequency band of 5.8 GHz [7].

Presently, there had been an upsurge in the interest of the automobile industries regarding wider applications of intra-vehicular wireless transmission. The use of wireless

communication in the vehicle cuts down the wiring harness, which will reduce the weight and cost of the car. It also eliminates the need of drilling to pass the cables, thereby improving robustness of the vehicle, and will simplify the design as well as production processes. As mentioned earlier, the IEEE 802.11p protocol was specified primarily for V2V/V2I scenarios where both transmitter and receiver are placed outside the vehicle [8]. In order to realize fully integrated intelligent transportation systems (ITSs), it is important to evaluate the efficacy of the protocol for wireless connections in in-car (both transmitter and receiver are inside the vehicle) and out-of-car (transmitter is inside, and receiver is outside, or vice-versa) scenarios as well.

1.2 Literature survey

There is a good number of open literature available that deal with vehicular channel measurement and modelling. We begin the list with [9], which provides a general review on advances and challenges in V2V channel measurement campaigns. The following papers, namely [10-12], describe measurement-based narrowband channel models for different situations: on highways, in cities, and on

*Correspondence: chandra@feec.vutbr.cz

¹Department of Radio Electronics, Brno University of Technology, Technicka 12, 61600 Brno, Czech Republic

Full list of author information is available at the end of the article

country roads. Different aspects of non-stationary vehicular channel measurements in the frequency band of our interest are addressed in [13,14]. Reports from some inter-vehicular measurement campaigns in the 5.9-GHz band are also made available in [15] and [16]. In particular, Cheng et al. [15] study the suitability of IEEE 802.11a for vehicular wireless links. Sen and Matolak [16] provide a wide set of power delay profile (PDP) measurements and proposed tapped delay line models based on Markov chains.

As far as intra-vehicular channel measurements are concerned, most of the articles are focused on ultra-wideband (UWB) operating over a broad frequency spectrum of 3 to 11 GHz. For example, the performance of multiband orthogonal frequency division multiplexing (MB-OFDM) in intra-car communication is studied by Maehara et al. [17]. In [18], Schack et al. report a comparison of broadband channel sounding experiments over a different range of cars. Another interesting paper is by Niu et al. [19], where they describe a detailed UWB channel modelling campaign for intra-vehicular environments. The characterization of the 5-GHz intra-vehicle communication channel is only attempted recently in [20], where the authors present power delay profiles, delay spread, and statistical channel models for a minivan and a bus.

Finally, in [21] and [22], the throughput and packet delivery performance of the IEEE 802.11p protocol is studied in V2V and V2I scenarios with different speeds of movement. However, to the best of our knowledge, none of the authors utilize the measured intra-vehicle channel models to evaluate the bit error rate (BER) for the IEEE 802.11p standard.

1.3 Contributions of the paper

In this paper, we present the results of intra-vehicle channel model measurements for the 5.8-GHz band for a typical passenger car. We provide measurements for a vehicle parked in an underground garage. The results were collected in the frequency domain by a vector network analyzer (VNA), then they were transformed into the time domain using the inverse fast Fourier transform (IFFT), and the large-scale variations (LSVs) from the measured PDPs were separated. The small-scale variations (SSVs), which were obtained after subtracting the LSV from the PDP, were characterized statistically thereafter. Finally, simulated BER results were obtained using a 802.11p simulation model. Specifically, the contributions of the paper are as follows:

- Results for intra-vehicle and out-of-vehicle single input single output (SISO) channel measurements performed in the 5.875- to 5.885-GHz frequency band.

- Characterization of the LSV trends via a two-term exponential decay model and the SSV random variations via logistic, normal, and generalized extreme value (GEV) distributions with the two-sample Kolmogorov-Smirnov (K-S) test.
- Comparison of PDP decay trends of UWB and 802.11p for an identical measurement setup.
- BER simulation for 802.11p using the measured channel data.

1.4 Organization of the paper

The paper reads as follows: Section 2 describes the measurement setup realized through a VNA. In Section , we provide a decay model to characterize the PDP, characterize the LSV trends, and find the optimal statistical distribution for the SSV. This section also includes a comparison between 802.11p and vehicular UWB channel characteristics. Next, the BER performance for the 802.11p standard is presented in Section 4. Finally, some conclusions are presented in Section 5.

2 Measurement setup

Measurements were performed with one transmitter (Tx) and three receiver (Rx) antennas in a right-hand, four-door Skoda Octavia car with dimensions: $4.659 \times 1.814 \times 1.462$ m. The vehicle was parked on the sixth floor in an underground garage of the Faculty of Electrical Engineering (FEKT), Brno University of Technology (VUT). Walls and floors of the garage premises are made of reinforced concrete, and they provide an environment that is free from narrowband interference. There were no parked cars on neighboring parking lots.

Figure 1a shows the underground garage and the parking lot with the car and equipments. The receive/ transmit antennas inside the car are zoomed in Figure 1b. The four omni-directional conical monopole antennas that were used are identical. The vertical polarization of the antennas can be confirmed from the radiation patterns presented in Figure 2 which depicts that the azimuth plane pattern is circular.

Equipments for recording data were placed outside of the vehicle. All doors and windows were closed, except the driver's window, which was slightly open to pass the cables between the antennas and the recording equipment.

For measuring and recording the transmission coefficient between transmitter and receiver, a four-port VNA from Agilent Technologies, E5071C (Agilent Technologies, Inc., Santa Clara, CA, USA) [7] was used (Figure 3 [bottom]). The transmit power was set at 5 dBm, and phase stable coaxial cables were used for interconnections. The VNA measures the complex valued channel transfer function in the frequency domain through the s -parameter, S_{x1} , which is the transmission coefficient between port 1 (Tx) and port $x \in \{2, 3, 4\}$ (Rx). The

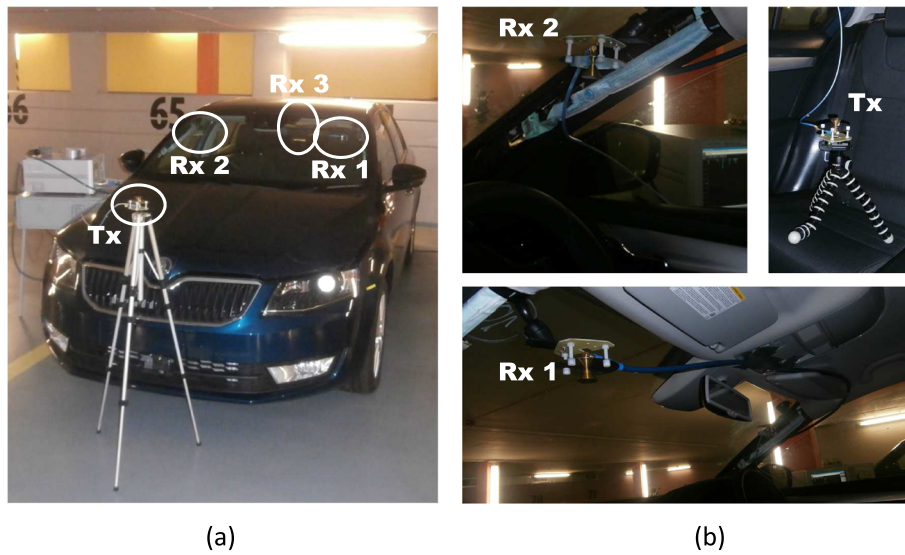


Figure 1 The underground parking lot and the receive/transmit antennas inside the car. (a) The vehicle under test. (b) Close up of the antennas inside the car.

measured frequency range (5.775 to 5.875 GHz) was swept with a frequency step size of $f_s = 0.125$ MHz. Due to the fine resolution in the frequency domain, we were able to construct the delay domain up to $t_d = 1/f_s = 8 \mu s$ without aliasing effect of the VNA. The information, when translated into the spatial domain, gives us a propagation space resolution $P_{sr} = c/BW = 3$ m and a maximum propagation distance of $L_{dmax} = c/f_s = 2.4$ km. The parameters, c and BW , denote propagation speed of electromagnetic waves in free space (3×10^8 m/s) and the bandwidth of the measured band, respectively.

The schematic diagram of the setup for IEEE 802.11p frequency domain channel sounding is presented in Figure 3 [top] [23]. Real and imaginary parts of the transfer function (S_{x1}) were exported to MATLAB. The frequency domain data over the entire bandwidth $BW = 100$ MHz

were partitioned into 10 MHz bins, where each bin corresponds to a sub-channel of 802.11p. All results were transformed from the frequency domain into the time domain, $h(\tau) = \mathcal{F}^{-1}H(f)$, utilizing the IFFT with a typical rectangular window. The PDP was calculated by averaging over ten sub-channel time-domain data.

Figure 4 shows transmitter and receiver antenna positions. A total of 15 different Tx-Rx combinations were tested with separations ranging from 0.53 to 3.38 m. The Tx antenna was placed at three different locations inside the vehicle and at two locations outside the vehicle. In-car Tx antenna positions were set at the right rear seat, armrest in the middle of the car, driver seat, while for locations outside the car, two positions at a height of 1.09 m were chosen: one in front of the car and the other one near the right headlamp. The Rx antennas were installed

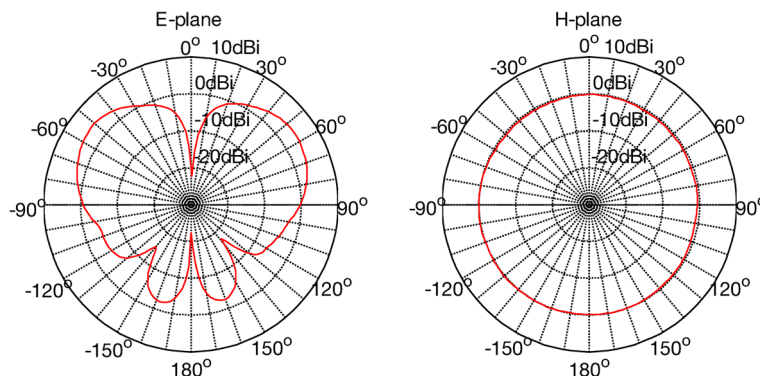


Figure 2 Simulated gain pattern of the conical antennas for central frequency of 5.8 GHz.

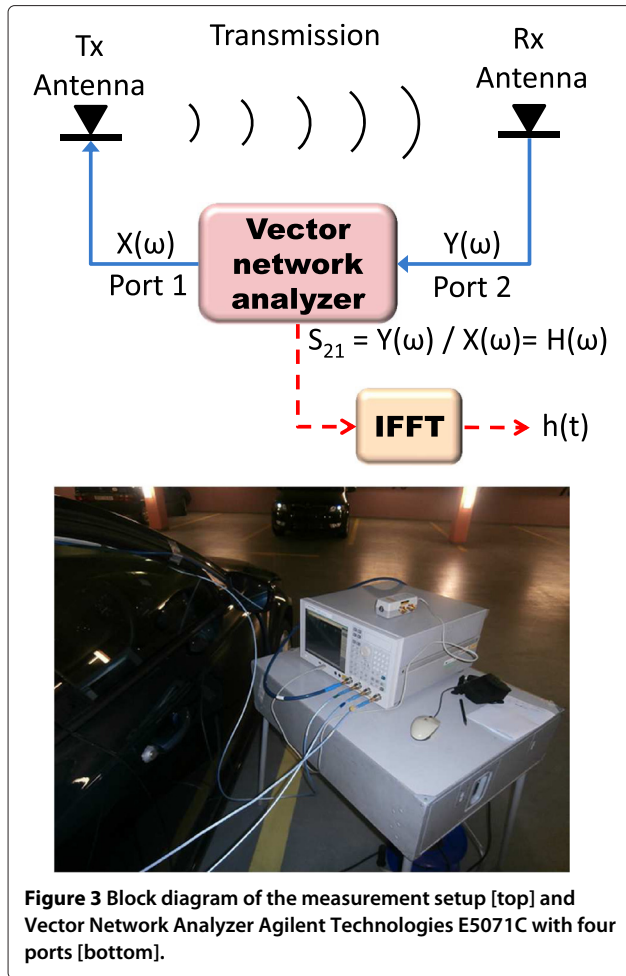


Figure 3 Block diagram of the measurement setup [top] and Vector Network Analyzer Agilent Technologies E5071C with four ports [bottom].

on the left and right upper edges of the windshield and on the roof in the rear part of the vehicle. The positions of antennas were chosen for realizing both line-of-sight (LOS) and non-line-of-sight (NLOS) scenarios. All these combinations are described in detail in Table 1.

3 Channel description

The measured channel impulse response (CIR) is $h(\tau) = h_{ch}(\tau) * h_{fil}(\tau)$ where $h_{ch}(\tau)$ refers to the actual channel response, $*$ denotes time-domain convolution, and $H_{Fil}(f) = \mathcal{F}\{h_{fil}(\tau)\}$ is the transfer function of the windowing operation. The band-limiting post-processing, however, does not lead to any serious causality issues [24]. The generic multipath CIR is described by:

$$h_{ch}(\tau) = \sum_{i=0}^{N-1} a_i \exp(j\theta_i) \delta(\tau - \tau_i) \quad (1)$$

where τ_i is the propagation delay, $a_i \exp(j\theta_i)$ is the complex amplitude coefficient of the i th multipath component, $\delta(\cdot)$ is the Dirac delta function, and N is the total number of multipath components.

The PDP is simply the squared channel impulse response $P(\tau) = |h(\tau)|^2$, and it includes LSV and SSV, which can be designated mathematically in the following manner: $P(\tau) = \gamma(\tau) + \xi(\tau)$, where $\gamma(\tau)$ denotes LSV and $\xi(\tau)$ is the SSV.

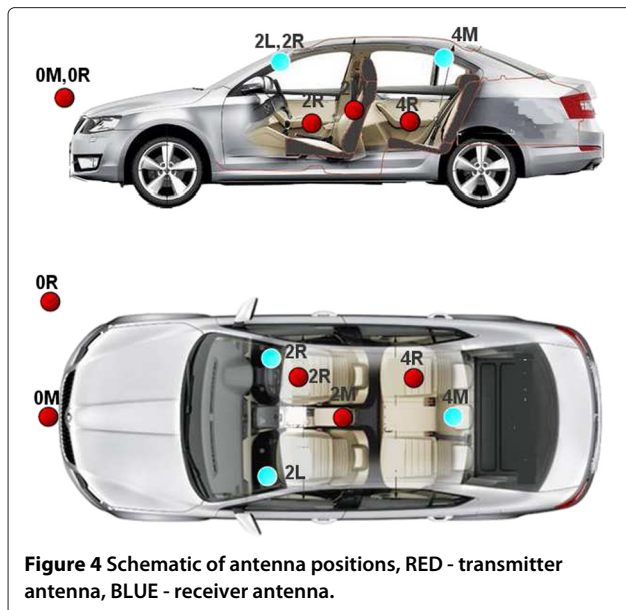


Figure 4 Schematic of antenna positions, RED - transmitter antenna, BLUE - receiver antenna.

Table 1 Detailed settings for measurements (Tx and Rx legends are shown in Figure 4)

Measurement number	Tx-Rx separation (m)	Tx position	Rx position	Remarks
1	0.53	2R	2R	LOS
2	0.69	4R	4M	LOS
3	0.74	2M	2L	LOS
4	0.85	2M	2R	LOS
5	0.87	2M	4M	LOS
6	0.94	2R	2L	LOS
7	1.26	4R	2R	NLOS
8	1.28	2R	4M	NLOS
9	1.41	4R	2L	NLOS
10	1.86	0R	2L	Tx at an angle
11	2.03	0M	2L	Tx in front
12	2.08	0M	2R	Tx in front
13	2.74	0R	2R	Tx at an angle
14	3.15	0R	4M	Tx at an angle
15	3.38	0M	4M	Tx in front

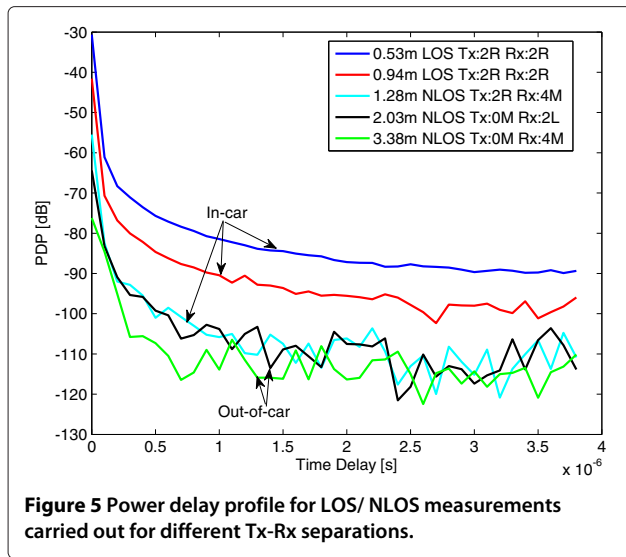


Figure 5 Power delay profile for LOS/ NLOS measurements carried out for different Tx-Rx separations.

Figure 5 shows the measured PDP for different LOS and NLOS conditions for both inside and outside of the vehicle. As expected, the power levels are significantly higher for the LOS measurements compared to the NLOS situations. The power levels for the NLOS case show rapid variations near the noise floor (−110 dB).

3.1 Large-scale variations

Analytical calculations performed for closed spaces [25,26] demonstrated an exponential decay of the PDP. As intra-vehicular channels appear to have similar signal propagation environments, we express the LSV with a two-term exponential model:

$$\gamma(\tau) = A \exp(B\tau) + C \exp(D\tau) \quad ; 0 < \tau < t_d/2. \quad (2)$$

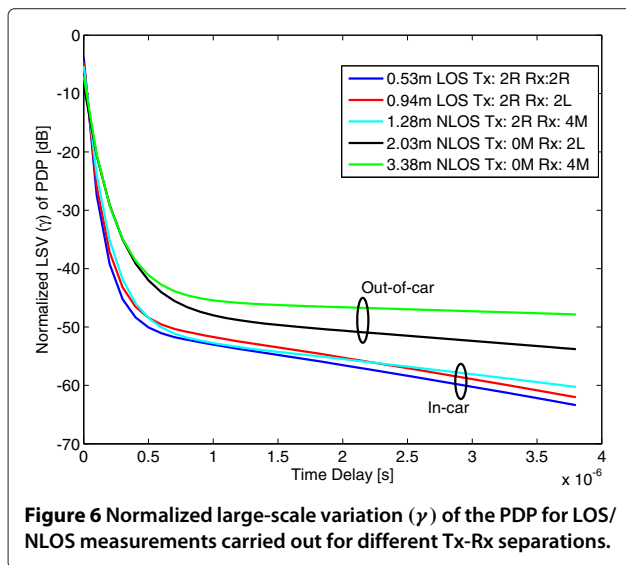


Figure 6 Normalized large-scale variation (γ) of the PDP for LOS/ NLOS measurements carried out for different Tx-Rx separations.

Table 2 Parameter values for LSV

Tx-Rx separation (m)	Parameter values			
	A	B ($\times 10^4$)	C	D ($\times 10^5$)
0.53	−49.81	0.63	45.98	−7.05
0.94	−48.56	0.64	43.89	−6.47
1.28	−50.66	0.46	45.37	−5.20
2.03	−47.36	0.34	38.82	−3.68
3.38	−45.32	0.14	38.25	−4.28

The first term includes power from direct and major reflected rays, and the second term, with a very low slope (close to linear), reflects the power from diffused multipath components. This exponential model (2) offers more flexibility compared to single-term exponential or linear models. Further, it also avoids discontinuities in the extracted LSVs, which are present when one attempts to divide the PDP into two (or more) delay parts and tries to fit individual expressions for each of these parts [27].

In order to evaluate how well the LSV model (2) corresponds to the actual PDP, we evaluated the mean square error (MSE) between the PDP and the LSV:

$$MSE = \frac{1}{M} \sum_{i=1}^M [P_i(\tau) - \gamma_i(\tau)]^2 \quad ; 0 < \tau < t_d/2. \quad (3)$$

The MSE is 6.59×10^{-5} , averaged over all the $M = 15$ measurements.

The LSVs for the two-term exponential model for different distance between Tx and Rx antennas of 0.53, 0.87, 1.28, 2.74, and 3.15 m are shown in Figure 6. It is observed that LSV for the LOS case drops more rapidly than for the NLOS scenario. This is in perfect harmony with earlier observations [28].

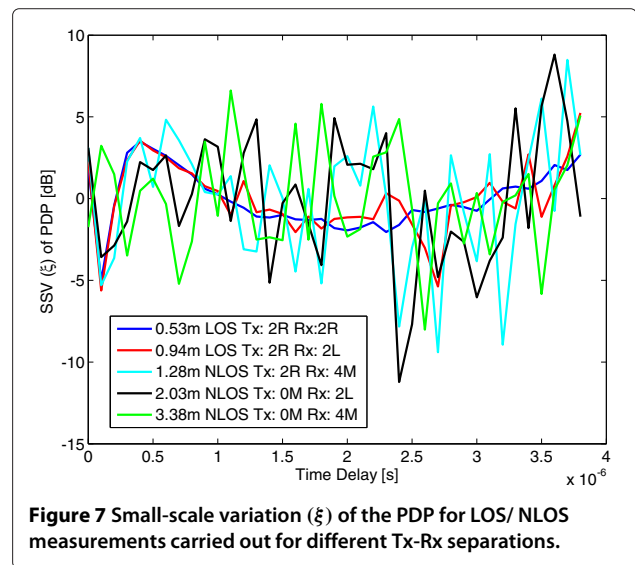


Figure 7 Small-scale variation (ξ) of the PDP for LOS/ NLOS measurements carried out for different Tx-Rx separations.

Table 3 Two sample K-S test p values for fitting SSV with different continuous distributions

Tx position	Tx-Rx separation (m)	Distributions		
		GEV	Logistic	Normal
In-car	0.53	0.3456	0.8838	0.7085
	0.94	0.8838	0.8838	0.7085
	1.28	0.7085	0.7085	0.8838
Out-of-car	2.03	0.9997	0.6297	0.5142
	3.38	0.8838	0.7085	0.8838

The parameters of the model for these five distances are given in Table 2. Both the coefficients, A and C , show similar values for in-car (or out-of-car) situations. On the other hand, the coefficient B decreases steadily with increasing Tx-Rx separation whereas D increases.

3.2 Small-scale variations

The SSV was obtained through subtracting the LSV from the measured PDP, i.e., $\xi(\tau) = P(\tau) - \gamma(\tau)$. Considering that the LSV follows (2), we separated SSVs for five different distances, and the results are depicted in Figure 7.

The characterization of the SSV is based on finding the appropriate random process using the normal, the logistic, and the GEV distributions. The GEV distribution [29] appeared to be a good fit for both UWB [30] and millimeter wave [31] small-scale variations. On the other hand, the logistic family of distributions [32] has been used successfully in ray-cluster-based modelling at 5 GHz [33] and modelling the probability density function (PDF) of the rms delay spread at 2.35 GHz [34]. We have also included the normal distribution as a reference. The PDF of these three distributions are given in (9), (10), and (11), respectively.

$$f(x|\mu, \sigma) = \frac{1}{\mu\sqrt{2\pi}} \exp\left[\frac{-(x - \mu)^2}{2\sigma^2}\right] \tag{4}$$

$$f(x|\mu, \sigma) = \frac{\exp\left(\frac{x-\mu}{\sigma}\right)}{\sigma \left[1 + \exp\left(\frac{x-\mu}{\sigma}\right)\right]^2} \tag{5}$$

$$f(x|k, \mu, \sigma) = \frac{1}{\sigma} \exp\left(-\beta^{-k-1}\right) \beta^{-1-k-1} \tag{6}$$

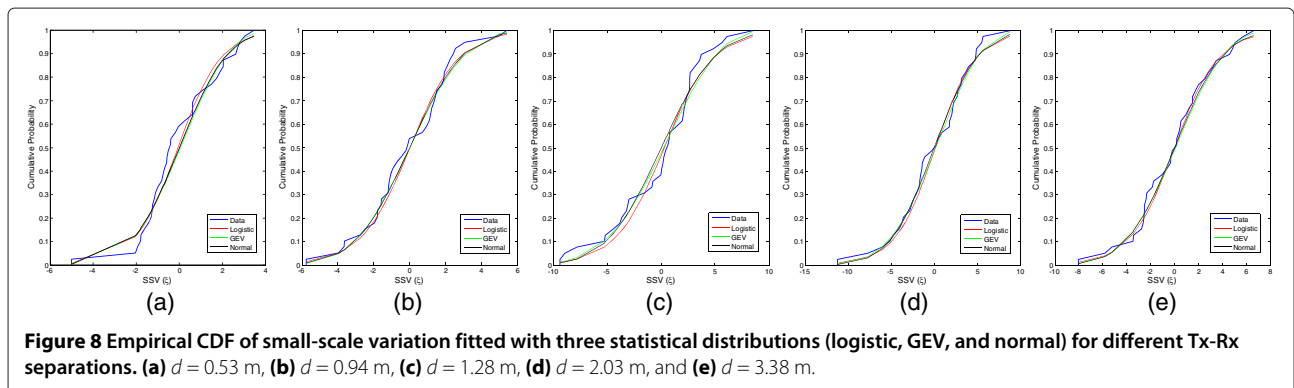
where $\beta = 1 + k\frac{x-\mu}{\sigma}$. The parameters, μ , σ , and k , are the location, scale, and shape parameters, respectively.

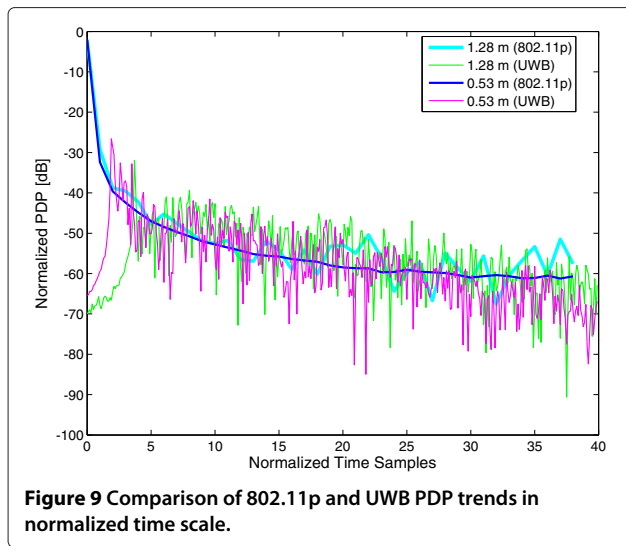
To compare distributions and SSV, we have performed the two-sample K-S test [35]. The p values are presented in Table 3. Higher p values for the logistic distribution inside the car and for the GEV distribution outside the car prove that they are the best candidates among the three for describing the SSV in in-car and out-of-car situations, respectively. The same can be observed from Figure 8, where the cumulative distribution functions (CDFs) of measured SSVs are fitted with these three distributions for results measured at different distances.

3.3 Comparison with UWB

UWB possesses a great potential for high-speed data communication and precise localization operations in cluttered closed-space hostile towards radio frequency (RF) signal propagation. Traditionally, the PDP for UWB channels are described with a modified Saleh-Valenzuela (S-V) model [19]. However, in a recent work by Demir et al. [36], the authors found that the PDP for UWB transmission in vehicular networks may be characterized by segmenting the PDP (in dB scale) into several linear slopes. Inspired by these facts, we tried to compare our results for 802.11p protocol with measurements for UWB (3 to 11 GHz) performed using the same VNA-based setup. The goal was to find if one can attain similar LSV trends in wider bandwidths as well.

The number of measured points was the same; however, due to the larger BW (8 GHz) and a frequency step size of $f_s = 100$ MHz, we have a smaller time range $t_d = 1/f_s = 10$ ns. Thus, we cannot compare the PDPs in an one-to-one basis. For analyzing LSV models, we use





a scaled comparison instead. For the UWB measurement, the propagation space resolution is $P_{sr} = 3$ cm and the maximum propagation distance is $L_{dmax} = 30$ m.

Figure 9 shows the UWB and the 802.11p normalized PDP vs normalized time samples. For UWB, it was found that the PDP constitutes one (or a few) major peaks followed by somewhat linear decreasing slope. The reader may also note the delay and lower power for the first peak of the UWB PDP. In addition, the delay and the maximum value of the peak is more for larger distances between the transmitting and receiving antennas. However, this phenomenon is not observed in narrowband 5.8 GHz measurements for 802.11p.

4 Simulation results

For BER simulation, we used MATLAB. A detailed description of the simulation methodology can be found in [37]. Parameters for generating the signal are available in [38]. A block-scheme diagram that corresponds to the SISO transmission model is presented in Figure 10.

The Tx generates 10^6 data sub-frames for a given energy per bit to noise power spectral density ratio (E_b/N_0). For signal transmission, we use rate 1/2 convolutional coding and BPSK modulation. On the receiver side, we use simple least square (LS) estimation and a hard Viterbi decoder. The 802.11p standard is based on OFDM with $N_{IFFT} = 64$ for a bandwidth of 10 MHz. In the time domain, each OFDM symbol contains 80 chips including a cyclic prefix of length 16. The final transmitted signal has a duration of $8 \mu s$.

Rician distribution had been successfully utilized for non-geometrical stochastic modelling of vehicular channels [11]. A Rician model also encompasses the Rayleigh model as a special case. For the channel block in Figure 10, the tap gains were calculated from the LSV based on a simple Rician model. The respective CIRs are shown in Table 4. It is interesting to find that real-life measurements exhibit a very fast decrease of the tap gains, similar to some earlier reports [39].

The BER results for different distances between Tx and Rx, for LOS and NLOS cases, and for intra-vehicle and out-of-vehicle situations are shown in Figure 11. Results can be classified quite unambiguously into two groups, one for intra-vehicle and the other for out-of-vehicle measurements. The BER worsens for higher Tx-Rx distance

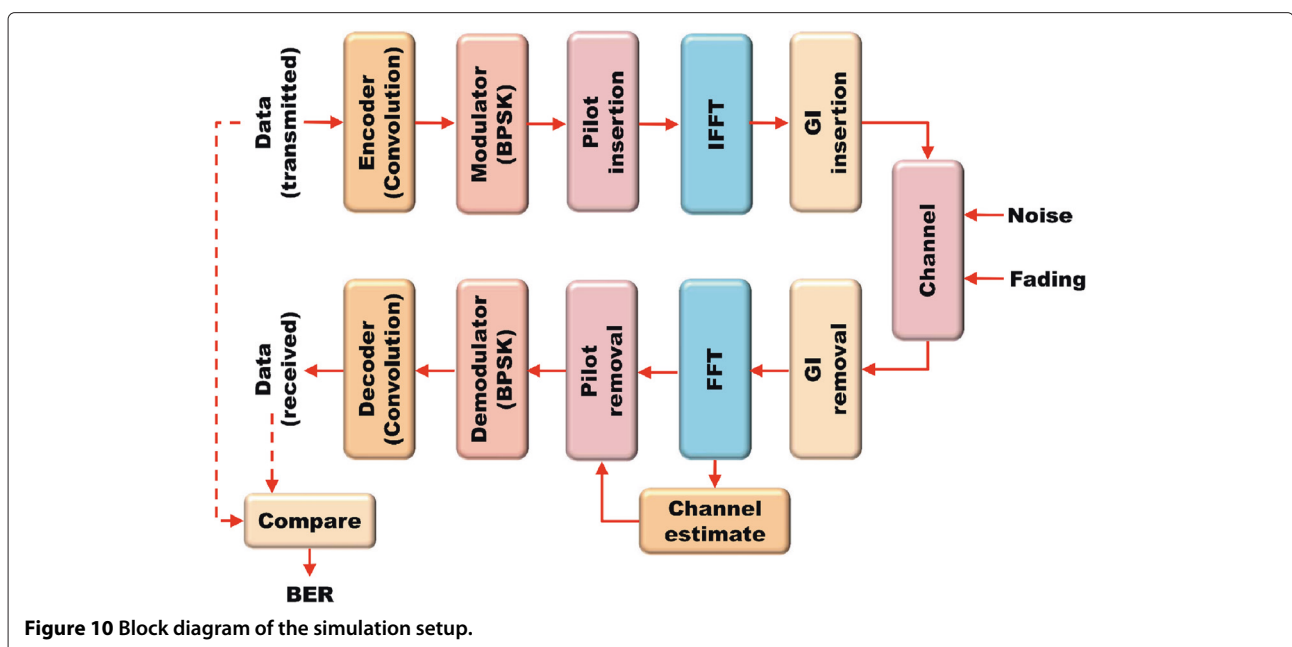


Table 4 Characteristics of the channel models

Tap delay (ns)	Tap gain (dB)				
	0.53 m LOS	0.94 m LOS	1.28 m NLOS	2.03 m NLOS	3.38 m NLOS
0	0	0	0	0	0
10	-11.78	-10.61	-9.61	-6.06	-6.69
20	-17.69	-16.24	-14.90	-10.28	-11.06
30	-20.69	-19.27	-18.27	-13.22	-13.93
40	-22.26	-20.93	-20.32	-15.28	-15.80
50	-23.11	-21.87	-21.58	-16.74	-17.04
60	-23.62	-22.45	-22.39	-17.76	-17.85
70	-23.95	-22.83	-22.91	-18.50	-18.40
80	-24.20	-23.10	-23.27	-19.04	-18.76
90	-21.41	-23.33	-23.53	-19.43	-19.01
K factor (dB)	21.30	20.07	19.61	15.15	15.40

inside the car, but outside the vehicle, the BER values almost remain unaffected when the Tx-Rx separation is altered. The BER results for intra-vehicle simulations are slightly better than the results for the out-of-vehicle channel. For a target BER of 10^{-5} , the required E_b/N_0 differs by 6 dB.

5 Conclusions

The aim of the text was to assess the suitability of protocol 802.11p for in-car wireless applications. For the purpose, extensive vehicular channel measurements in the 5.8-GHz band were carried out. A double exponential decay model was used for describing the basic trend of the measured PDP, and we utilized it for IEEE 802.11p BER simulation.

The BER achieves the recommended values for all variants of the channel, and it can be concluded that 802.11p standard (in particular, the PHY protocol stack) can be adopted for intra-vehicular communication systems.

Competing interests

The authors declare that they have no competing interests.

Acknowledgements

This work was supported by the SoMoPro II programme, Project No. 3SGA5720 *Localization via UWB*, co-financed by the People Programme (Marie Curie action) of the Seventh Framework Programme of EU according to the REA Grant Agreement No. 291782 and by the South-Moravian Region. The research is further co-financed by the Czech Science Foundation, Project No. 13-38735S *Research into wireless channels for intra-vehicle communication and positioning*, and by Czech Ministry of Education in frame of National Sustainability Program under grant LO1401. For research, infrastructure of the SIX Center was used. The generous support from Skoda a.s. Mlada Boleslav are also gratefully acknowledged.

Author details

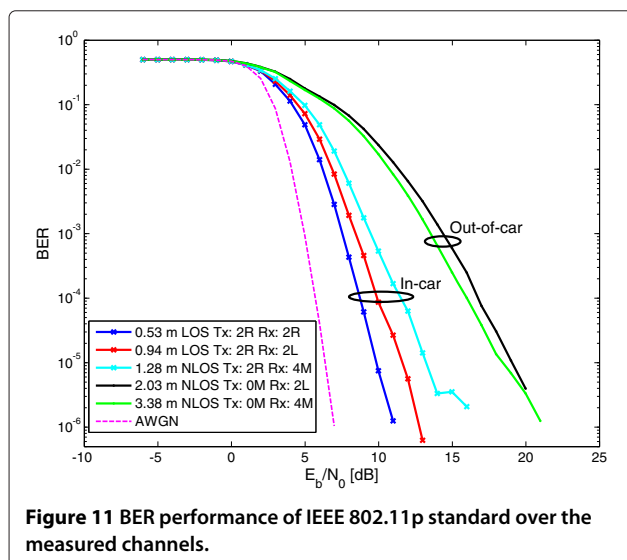
¹Department of Radio Electronics, Brno University of Technology, Technicka 12, 61600 Brno, Czech Republic. ²AIT Austrian Institute of Technology GmbH, 1220 Vienna, Austria. ³Telecommunications Research Center Vienna (FTW), Donau-City-Straße 1, 1220 Vienna, Austria. ⁴Institute of Telecommunications, Vienna University of Technology, Gusshausstraße 25, 1040 Vienna, Austria.

Received: 29 November 2014 Accepted: 9 February 2015

Published online: 10 March 2015

References

1. J Gozalvez, M Sepulcre, R Bauza, IEEE 802.11p vehicle to infrastructure communications in urban environments. *IEEE Commun. Mag.* **50**(5), 176–183 (2012)
2. M Faezipour, M Nourani, A Saeed, S Addepalli, Progress and challenges in intelligent vehicle area networks. *Commun. ACM.* **55**(2), 90–100 (2012)
3. H Hartenstein, KP Laberteaux, A tutorial survey on vehicular ad hoc networks. *IEEE Commun. Mag.* **46**(6), 164–171 (2008)
4. IEEE Computer Society, IEEE Standard for Information Technology - telecommunications and information exchange between systems - local and metropolitan area networks - specific requirements - part 11: wireless LAN medium access control (MAC) and physical layer (PHY) specifications amendment 6: wireless access in vehicular environments. *IEEE Std.* **802**, 1–51 (Jul. 2010). doi: 10.1109/IEEESTD.2010.5514475



5. Society IEEE Vehicular Technology, IEEE guide for wireless access in vehicular environments (WAVE) - architecture. IEEE Std. **1069**, P1609.0/D7.0, , 1–77 (Mar. 2014). <http://ieeexplore.ieee.org/servlet/opac?punumber=6576803>
6. CAR 2 CAR communication consortium: overview of the C2C-CC system. Manifesto, 1–94 (Aug. 2007). http://elib.dlr.de/48380/1/C2C-CC_manifesto_v1.1.pdf
7. M Muller, WLAN 802.11p Measurements for Vehicle to Vehicle (V2V) DSRC. Application note Rohde & Schwarz: 1 MA152_Oe, 1–25 (Sep. 2009). www.rohde-schwarz.cz/file/1MA152_2e.pdf
8. CF Mecklenbrauker, AF Molisch, J Karedal, F Tufvesson, A Paier, L Bernado, T Zemen, O Klemp, N Czink, Vehicular channel characterization and its implications for wireless system design and performance. *Proc. IEEE*. **99**(7), 1189–1212 (2011)
9. W Cheng-Xiang, C Xiang, DI Laurenson, Vehicle-to-vehicle channel modeling and measurements: recent advances and future challenges. *IEEE Commun. Mag.* **47**, 96–103 (2009)
10. A Paier, J Karedal, N Czink, H Hofstetter, C Dumard, T Zemen, F Tufvesson, CF Mecklenbrauker, AF Molisch, in *Proc. IEEE PIMRC*. First results from car-to-car and car-to-infrastructure radio channel measurements at 5.2 GHz (Athens, 2007), pp. 1–5
11. G Acosta-Marum, MA Ingram, Six time- and frequency-selective empirical channel models for vehicular wireless LANs. *IEEE Veh. Tech. Mag.* **2**, 4–11 (2007)
12. S Biswas, R Tatchikou, F Dion, Vehicle-to-vehicle wireless communication protocols for enhancing highway traffic safety. *IEEE Commun. Mag.* **44**, 74–82 (2006)
13. L Bernado, T Zemen, F Tufvesson, AF Molisch, CF Mecklenbrauker, Delay and Doppler spreads of non-stationary vehicular channels for safety relevant scenarios. *IEEE Trans. Veh. Tech.* **63**(1), 82–93 (2014)
14. L Bernado, T Zemen, F Tufvesson, AF Molisch, CF Mecklenbrauker, Time- and frequency-varying K-factor of non-stationary vehicular channels for safety-relevant scenarios. *IEEE Trans. Intell. Transport. Syst.* 1–11 (2015). doi: 10.1109/TITS.2014.2349364
15. L Cheng, BE Henty, R Cooper, DD Stancil, F Bai, A measurement study of time-scaled 802.11a waveforms over the mobile-to-mobile vehicular channel at 5.9 GHz. *IEEE Commun. Mag.* **46**(5), 84–91 (2008)
16. I Sen, DW Matolak, Vehicle-vehicle channel models for the 5-GHz band. *IEEE Trans. Intell. Transport. Syst.* **9**(2), 235–245 (2008)
17. F Maehara, R Kaneko, A Yamakita, S Goto, in *Proc. IEEE CSNDSP*. Coverage performance of MB-OFDM UWB in-car wireless communication (Newcastle upon Tyne UK, 2010), pp. 417–421
18. M Schack, R Geise, I Schmidt, R Piesiewicz, T Kurner, in *Proc. IEEE EuCAP*. UWB channel measurements inside different car types (Berlin, Germany, 2009), pp. 640–644
19. W Niu, J Li, T Talty, Ultra-wideband channel modeling for intravehicle environment. *EURASIP J. Wirel. Commun. Net.* **2009**(806209), 1–12 (2009)
20. DW Matolak, A Chandrasekaran, in *Proc. IEEE VTC*. 5 GHz intra-vehicle channel characterization (Quebec City, QC, 2012), pp. 1–5
21. M Wellens, B Westphal, P Mahonen, in *Proc. IEEE VTC*. Performance evaluation of IEEE 802.11-based WLANs in vehicular scenarios (Dublin, 2007), pp. 1167–1171
22. FA Teixeira, VF e Silva, JL Leoni, DF Macedo, JMS Nogueira, Vehicular networks using the IEEE 802.11p standard: an experimental analysis. *Vehic. Commun.* **1**(2), 91–96 (2014)
23. M Jankiraman, *Space-Time Codes and MIMO Systems*. (Artech House, Boston, London, 2004)
24. P Pupalaiakis, in *Proc. DesignCon*. The relationship between discrete frequency s-parameters and continuous frequency responses (UBM, 2012)
25. J Hansen, M Nold, in *Proc. IEEE GLOBECOM*. Analytic calculation of the power delay profile for single room wireless LAN environments, vol. 1 (San Francisco, CA, USA, 2000), pp. 98–102
26. J Hansen, An analytical calculation of power delay profile and delay spread with experimental verification. *IEEE Commun. Lett.* **7**(6), 257–259 (2003)
27. H Yang, P Smulders, M Herben, Channel characteristics and transmission performance for various channel configurations at 60 GHz. *EURASIP J. Wirel. Commun. Net.* **2007**(19613), 1–15 (2007)
28. S Guerin, YJ Guo, SK Barton, in *Proc. IEEE ICAP*. Indoor propagation measurements at 5 GHz for HIPERLAN, vol. 2 (Edinburgh, UK, 1997), pp. 306–310
29. S Kotz, S Nadarajah, *Extreme Value Distributions: Theory and Applications*. (Imperial College Press, London, UK, 2000)
30. J Blumenstein, T Mikulasek, R Marsalek, A Chandra, A Prokes, T Zemen, C Mecklenbrauker, in *IEEE VNC*. In-vehicle UWB channel measurement, model and spatial consistency (Paderborn, Germany, 2014), pp. 77–80
31. J Blumenstein, T Mikulasek, R Marsalek, A Prokes, T Zemen, C Mecklenbrauker, in *Proc. IEEE VTC*. In-vehicle mm-wave channel model and measurement (Vancouver, Canada, 2014), pp. 1–5
32. N Balakrishnan, VB Nebzorov, *A Primer on Statistical Distributions*. (John Wiley and Sons, New York, USA, 2003)
33. H El-Sallabi, DS Baum, P Zetterberg, P Kyosti, T Rautiainen, C Schneider, in *Proc. IEEE VTC*. Wideband spatial channel model for MIMO systems at 5 GHz in indoor and outdoor environments, vol. 6 (Melbourne, Australia, 2006), pp. 2916–2921
34. Y Guo, J Zhang, C Tao, L Liu, L Tian, Propagation characteristics of wideband high-speed railway channel in viaduct scenario at 2.35 GHz. *J Modern Transportation*. **20**(4), 206–212 (2012)
35. FJ Massey, The Kolmogorov-Smirnov test for goodness of fit. *J. Am. Statist. Assoc.* **46**(253), 66–78 (1951)
36. U Demir, CU Bas, SC Ergen, Engine compartment UWB channel model for intravehicular wireless sensor networks. *IEEE Trans. Veh. Tech.* **63**(6), 2497–2505 (2014)
37. P Kukolev, Comparison of 802.11a and 802.11p over fading channels. *Elektrorevue*. **4**(1), 7–11 (2013)
38. P Kukolev, in *Proc. Radioelektronika*. BER performance of 802.11p standard over an ITU-R multipath channel (Pardubice, Czech Republic, 2013), pp. 391–396
39. A Paier, *The vehicular radio channel in the 5 GHz band*. PhD Thesis. (Technischen Universität Wien, Vienna, Austria, 2010)

Submit your manuscript to a SpringerOpen® journal and benefit from:

- Convenient online submission
- Rigorous peer review
- Immediate publication on acceptance
- Open access: articles freely available online
- High visibility within the field
- Retaining the copyright to your article

Submit your next manuscript at ► springeropen.com